Microscopic Surface Patterns of a Liquid Crystalline Polyacrylate Film**

By *Daniel Sentenac*, *Boris I. Ostrovskii*, and *Wim H. de Jeu**

Progress in miniaturization with conventional lithographic techniques has now reached a critical limit that is increasingly difficult to improve upon. In the meantime, new techniques have emerged that are able to reduce the size of simple features down to molecular dimensions. Among these, molecular printing or embossing from polymeric materials can create simple features with sizes well below 0.1 μm. An easy-to-process variation is polymeric self-assembly[1] in which the resulting microstructures can be uniformly orientated by electric fields[2] or specific surface fields.[3] Subsequent simple photochemical treatment leads to well-defined periodic arrays of nanoporous materials.[4] In this context side-chain liquid crystalline (LC) polymers are an interesting variety of polymer, composed of liquid crystalline molecules (mesogens) that are laterally grafted onto a classical polymer backbone. Their properties depend on the delicate interactions between mesogenic ordering and polymer entropy.[5] They represent a unique class of material with viscoelastic and mesomorphic behavior that leads to interesting macroscopic properties including specific wettability, tackiness,[6] and (anti)ferroelectricity.[7] Incorporation into block copolymers gives a "tandem" interaction of competing ordering at different length scales: the microphase separation between the two polymer blocks and the LC ordering inside one of the blocks. This possibility has been exploited to orient a lamellar phase of a hybrid smectic LC/amorphous block copolymer perpendicularly onto a homogeneous float glass substrate.[8] In this report we show that lamellae-like surface ripples on a nanometer scale can be induced in LC polyacrylate films on a homogeneous substrate. The film surface shows regular height modulations with a periodicity of 9 nm, which are attributed to a coupling between local LC order and surface curvature energy.[9]

The phase diagram poly(4-(5-acryloyloxypent-1-yloxyphenyl)-4′-butoyloxybenzoate) (PABB-5) homopolymer[10] is shown in Figure 1. We prepared two types of film characterized by a degree of polymerization $N = 37$ (film I) and $N = 55$ (film II), respectively. Common to both samples is the presence of a nematic phase at high temperatures and a C⁻ phase

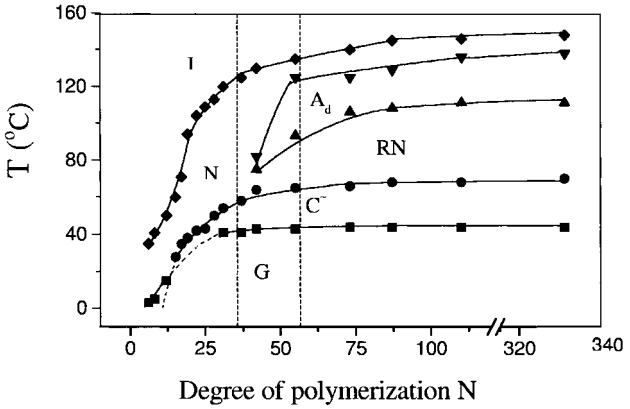

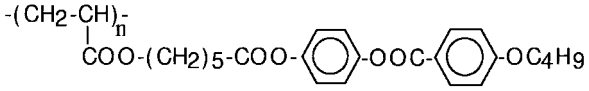

Fig. 1. Structural formula and phase diagram of the LC polyacrylate PABB-5 [10]. I, N, Sm-A_d, RN, C⁻, and g stand for isotropic, nematic, smectic-A_d, reentrant nematic, C⁻ phase and glassy state, respectively (see text). The two samples studied as thin films are indicated.

at low temperatures. In sample II this situation is reached via an intermediate smectic-A_d phase (Sm-A_d) and a reentrant nematic phase. The liquid layers in the Sm-A_d phase are formed by partially overlapping side-groups, giving a periodicity incommensurate with the length of a mesogenic side group. The C⁻ phase consists of a two-dimensional oblique lattice of side chains, which are arranged in chevron-like blocks of "almost bilayers". Liquid-like order is retained in the third dimension. Evidently two competing length scales are present in the system, leading to the frustrated phase behavior of Figure 1. Hence the phase transformations have a steric (entropic) origin and are driven by changes of the polymer backbone conformation, which become more pronounced for long chains. Films of composition I and II and a thickness between 20 and 90 nm were investigated by specular X-ray reflectivity (XRR), while direct real-space images were obtained by atomic force microscopy (AFM).

For film I, annealed in the nematic phase at 85 °C, XRR indicates the presence of surface-induced layering as revealed by the weak broad bump at $q_z \approx 3.6$ nm^{-1} decorated by interference fringes from the two limiting surfaces (Fig. 2a). The best fit to the data indicates an essentially uniform density distribution in the interior of the film and two additional top layers of about 4 nm. The AFM surface topography reveals a network of micrometric elongated asperities of irregular heights around 4.5 nm (Fig. 3). Zooming in on the surface of film I we observe a remarkable well-defined lateral lamellar structure on the nanometer scale (Fig. 4). The lamellae are oriented along the direction of the elongated asperities. The surface ripples stem from a regular height deformation of 0.4–0.5 nm. The average in-plane periodicity is long-range as demonstrated by the fast Fourier transform (FFT) of the direct image, which shows two orders of Bragg peaks (Fig. 4d). After annealing film II in the smectic phase, XRR

[*] Prof. W. H. de Jeu, Dr. D. Sentenac
FOM-Institute for Atomic and Molecular Physics
Kruislaan 407, NL-1098 SJ Amsterdam (The Netherlands)
E-mail: dejeu@amolf.nl
Dr. B. I. Ostrovskii
Institute of Crystallography, Academy of Science of Russia
Leninski pr. 59, Moscow 117333 (Russia)

[**] We thank N. I. Boiko and V. P. Shibaev for the synthesis of the polymers and for valuable discussions. This work is part of the research program of the "Stichting voor Fundamenteel Onderzoek der Materie" (Foundation for the Fundamental Research of Matter, FOM), which is financially supported by the "Nederlandse Organisatie voor Wetenschappelijk Onderzoek" (Netherlands Organization for the Advancement of Research, NWO). DS acknowledges support from the TMR-Program of the European Union (ERBFMICT 9828877).

  0935-9648/01/1407-1079 $ 17.50+.50/0

ADVANCED MATERIALS

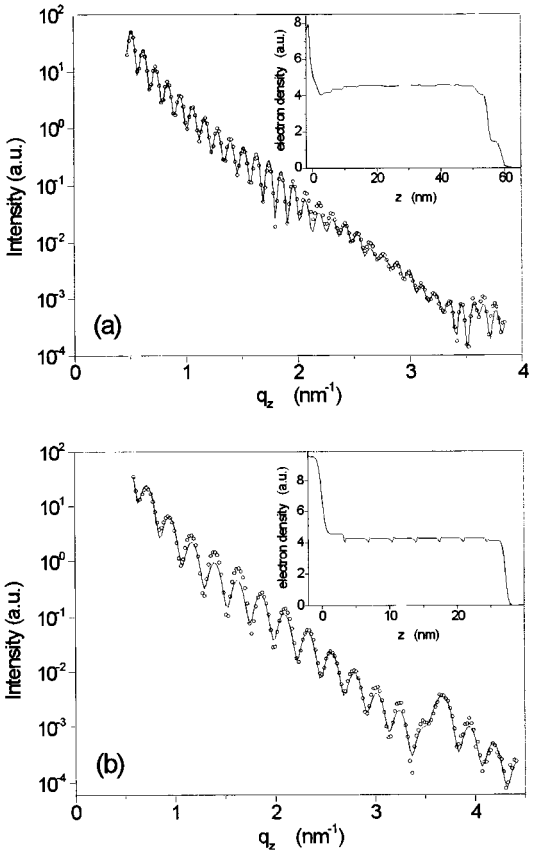

Fig. 2. XRR of film I (a) and II (b) after annealing in the nematic phase (I, T = 85 °C) and in the Sm-A_d phase (II, T = 105 °C), respectively. The solid line through the data points gives the best fit corresponding to the electron density profile in the inset with the substrate at z = 0. In (a) the weak broad bump around q_z = 3.6 nm^{-1} indicates surface-induced lamellar ordering with an average thickness of ~4 nm.

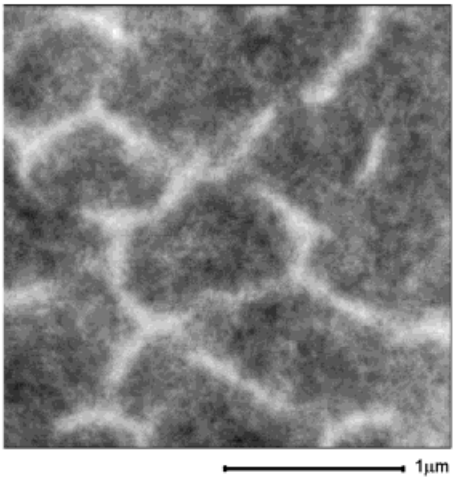

Fig. 3. AFM topography (2.5 × 2.5 μm^2) of film I showing a two-dimensional network of elongated asperities of irregular heights around 4.5 nm.

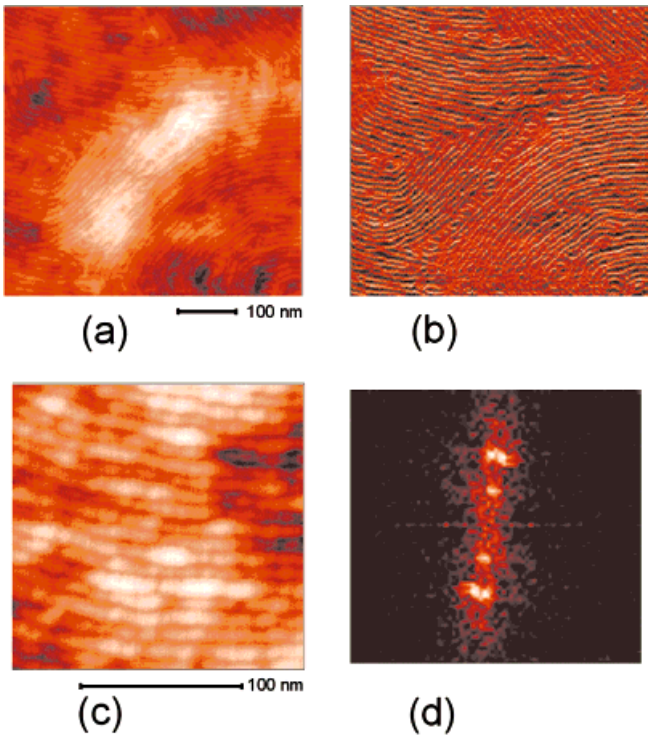

Fig. 4. Details of the surface patterns of film I at larger magnification. a) AFM topography (500 × 500 nm^2) of the surface lamellae oriented along an elongated asperity, and b) AFM phase image corresponding to the same area with enhanced contrast between consecutive lamellae. c) Local details of the surface ripples (180 × 180 nm^2) and d) corresponding fast Fourier transform. The average wavelength of the ripples is ~9 nm; the average height difference between two lamellae is ~0.4–0.5 nm.

In an attempt to understand these observations we concentrate on the two stable types of periodicity in the PABB-5 series as observed in bulk X-ray measurements[10] and schematically illustrated in Figure 5. The first one of 3.5 nm corresponds to an interdigitated structure of the side-chain mesogens and determines the layer spacing in the Sm-A_d

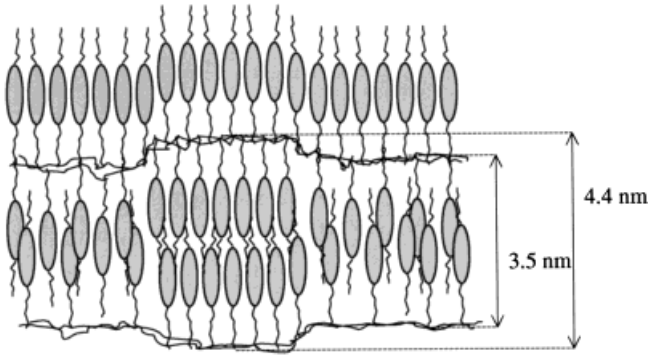

Fig. 5. Schematic representation of the two types of layer spacing with different degrees of overlapping side chains, contributing to the top layer undulations.

reveals stacks of smectic layers parallel to the substrate (Fig. 2b). On top of this film again regular lamellae with a lateral periodicity of 9 nm are observed, similar as shown in Figure 4 for film I in the nematic phase. Hence the nano-ripples seem to be a material property rather than a phase property.

phase. The second one of 4.4 nm condenses in the C^- phase and is also found as short-range structure up to high temperatures in the nematic phase of sample I. Interestingly, the thickness of the surface-induced layers of film I matches with an average of the two stable bulk periods, and the asperity

  0935-9648/01/1407-1080 $ 17.50+.50/0

height with the larger $C^{\sim}$ spacing. For this film we noted with decreasing temperature a progressive dewetting of the polymer film resulting in the formation of macroscopic holes once the $C^{\sim}$ phase is reached. Hence we speculate that the top network of asperities might originate from the initial stages of dewetting of surface-induced pre-transitional $C^{\sim}$-domains.

The origin of the nanometer-scale lateral surface lamellae seems to be complicated. They have characteristics close to those of the ripple phase of lipid membranes. Such membranes consist of bilayers of amphiphilic molecules with their hydrocarbon tails shielded from the surrounding water. They are flexible and may form phases with a periodic surface corrugation on the scale of 10–20 nm.[11] Surface ripples in a film can arise due to a coupling between surface curvature and some local internal variable, which may be as different as hydrocarbon chain conformation, tilt angle, or local composition.[9] In the frustrated PABB-5 series with competing length scales, the local order is naturally represented by an order parameter describing the degree of overlap of the mesogenic side chains. Such a phenomenological model has been elaborated and will be published elsewhere.[12] Using typical LC polymer parameters it predicts an undulation period of the ripples of the order of 10–100 nm, qualitatively in agreement with our observations. Hence we assume that the surface ripples originate from the competition between the two stable side-chain packing configurations with a spacing of 3.5 and 4.4 nm, which at the film surface is accommodated by film curvature. In agreement with this picture the amplitude of the surface ripples (0.4–0.5 nm) corroborates with half the difference of these two spacings.

Compared to other side-chain LC systems, the present PABB-5 series seems to be unique in displaying the reported surface-induced nano-ripples. The phase diagram suggests that this is due to two competing lengths scales at almost equal free energy. To investigate this relation, systematic chemistry is required varying the length of the mesogenic end chains as well as the spacer group connecting the mesogens to the polymer backbone. This might also be the route to vary the periodicity of the lateral surface ripples. A second challenge is to employ external fields to force uniformity over larger areas.

In conclusion we have reported an easy and straightforward way to pattern a homogeneous surface laterally by using the specific self-organizing properties of a side-chain LC polyacrylate. Incorporation of this type of LC polyacrylate in block copolymers may open additional new ways to realize multiple length scale lateral patterning.

Experimental

The samples (polydispersity $M_w/M_n \approx 1.1$) were prepared by spin coating a toluene solution onto a float glass substrate. Film thicknesses from 20 to 90 nm were tuned by changing the spinning velocity (1500–3000 rpm) and the polymer concentration (6–14 mg/mL). The films were annealed overnight in a dry nitrogen atmosphere at a temperature in the specific LC phase chosen, where also the XRR was performed. AFM was carried out on films frozen into the glassy state by quenching to room temperature.

XRR was performed at a wavelength $\lambda = 0.154$ nm (Cu Kα line from a 18 kW rotating anode generator) using a triple-axis reflectometer [13]. The incident beam was monochromatized and focused in the direction perpendicular to the scattering plane by a bent graphite (002) crystal. In reciprocal space, the specularly scattered intensity is a function of $q_z = (4\pi/\lambda)\sin\theta$, where θ is the angle of incidence and the z-axis is perpendicular to the film. $I(q_z)$ is analysed rigorously through the use of an optical formalism [14] and convoluted with the experimental resolution of $\Delta q_z = 0.04$ nm^{-1}. The films are modeled by a succession of parallel homogeneous slabs, each of them characterized by three parameters: thickness, density, and interfacial roughness described by Gaussian statistics.

A Solver atomic force microscope (NT-MDT, Zelenograd, Moscow) was employed in the resonant mode using standard probes with a tip of ~10 nm radius and a cantilever resonant frequency of ~300 kHz.

Received: November 24, 2000
Final version: February 25, 2001

[1] Y. Xia, J. A. Rogers, K. E. Paul, G. Whitesides, *Chem. Rev.* **1999**, *99*, 1823.
[2] a) E. Schäffer, T. Thurn-Albrecht, T. P. Russell, U. Steiner, *Nature* **2000**, *403*, 874. b) T. L. Morkved, M. Lu, A. M. Urbas, E. E. Ehrichs, H. M. Jaeger, P. Mansky, T. P. Russell, *Science* **1996**, *273*, 931.
[3] a) L. Rockford, Y. Liu, P. Mansky, T. P. Russell, M. Yoon, S. G. J. Mochrie, *Phys. Rev. Lett.* **1999**, *82*, 2602. b) A. M. Higgins, R. A. L. Jones, *Nature* **2000**, *404*, 476. c) P. Mansky, Y. Liu, E. Huang, T. P. Russell, C. J. Hawker, *Science* **1997**, *275*, 1458.
[4] a) M. Park, C. Harrison, P. M. Chaikin, R. A. Register, D. H. Adamson, *Science* **1997**, *276*, 1401. b) T. Thurn-Albrecht, R. Steiner, J. DeRouchey, C. M. Stafford, E. Huang, M. Bal, M. Tuominen, C. J. Hawker, T. P. Russell, *Adv. Mater.* **2000**, *12*, 787.
[5] See, for example, V. P. Shibaev, L. Lam, *Liquid Crystalline and Mesomorphic Polymers*, Springer, New York **1994**.
[6] G. de Crevoisier, P. Fabre, J.-M. Corpart, L. Leibler, *Science* **1999**, *285*, 1246.
[7] a) V. P. Shibaev, M. V. Kozlovsky, L. A. Beresnev, L. M. Blinov, N. A. Plate, *Polym. Bull.* **1984**, *12*, 299. b) E. A. S. Bustamante, S. V. Yablonskii, B. I. Ostrovskii, L. A. Beresnev, L. M. Blinov, W. Haase, *Chem. Phys. Lett.* **1996**, *260*, 447. c) K. M. Blackwood, *Science* **1996**, *273*, 909.
[8] G. C. L. Wong, J. Commandeur, H. Fischer, W. H. de Jeu, *Phys. Rev. Lett.* **1996**, *77*, 5221.
[9] a) S. Leibler, D. Andelman, *J. Phys.* **1987**, *48*, 2013. b) C.-M. Chen, T. C. Lubensky, F. C. Mackintosh, *Phys. Rev. E* **1995**, *51*, 504.
[10] N. I. Boiko, V. P. Shibaev, B. Ostrovskii, S. N. Sulyanov, D. Wolff, J. Springer, *Macromol. Chem. Phys.* **2001**, *202*, 297.
[11] a) A. N. Zasadzinski, J. Schneir, J. Gurley, V. Elings, P. K. Hansma, *Science* **1988**, *239*, 1013. b) J. T. Woodward, J. A. Zasadzinski, *Phys. Rev. E* **1996**, *53*, 3044.
[12] B. I. Ostrovskii, D. Sentenac, I. I. Samoilenko, W. H. de Jeu, unpublished.
[13] E. A. L. Mol, J. D. Shindler, A. N. Shalaginov, W. H. de Jeu, *Phys. Rev. E* **1996**, *54*, 536.
[14] a) L. G. Parrat, *Phys. Rev.* **1954**, *95*, 359. b) M. Tolan, *X-ray Scattering from Soft Matter Thin Films*, Springer, Berlin **1999**.

Sintering of Nanocrystalline CeO_2 Ceramics**

By *Christoph Kleinlogel* and *Ludwig J. Gauckler**

Ceria solid solutions exhibit a 4 to 5 times higher ionic conductivity at intermediate temperatures (600–700 °C) compared to zirconia.[1] Therefore solid oxide fuel cells with ceria electrolytes can be operated at temperatures as low as 700 °C

[*] Prof. L. J. Gauckler, Dr. C. Kleinlogel
Department of Materials
Swiss Federal Institute of Technology, ETH Zurich
Sonneggstr. 5, CH-8092 Zurich (Switzerland)
E-mail: gauckler@nonmet.mat.ethz.ch

[**] The authors thank G. Kostorz and F. Kral from the Institute for Applied Physics, ETH-Zurich, for the TEM micrographs and G. Bayer for helpful comments. Financial support from the Swiss Priority Program on Materials (PPM) of the board of the Swiss Federal Institutes of Technology is gratefully acknowledged.

  0935-9648/01/1407-1081 $ 17.50+.50/0